Simplest piston problem. I. Elastic collisions

Pablo I. Hurtado[1,2,*] and S. Redner[3,†]
[1]*Institute Carlos I for Theoretical and Computational Physics, Universidad de Granada, 18071 Granada, Spain*
[2]*Department of Physics, Boston University, Boston, Massachusetts 02215, USA*
[3]*Theoretical Division and Center for Nonlinear Studies, Los Alamos National Laboratory, Los Alamos, New Mexico 87545, USA*
(Received 28 July 2005; published 27 January 2006)

We study the dynamics of three elastic particles in a finite interval where two light particles are separated by a heavy "piston." The piston undergoes surprisingly complex motion that is oscillatory at short time scales but seemingly chaotic at longer scales. The piston also makes long-duration excursions close to the ends of the interval that stem from the breakdown of energy equipartition. Many of these dynamical features can be understood by mapping the motion of three particles on the line onto the trajectory of an elastic billiard in a highly skewed tetrahedral region. We exploit this picture to construct a qualitative random walk argument that predicts a power-law tail, with exponent $-3/2$, for the distribution of time intervals between successive piston crossings of the interval midpoint. These predictions are verified by numerical simulations.

DOI: 10.1103/PhysRevE.73.016136 PACS number(s): 02.50.Ey, 05.20.Dd, 45.05.+x, 45.50.Tn

I. INTRODUCTION

A classic thermodynamics problem is the adiabatic "piston" [1], where a gas-filled container is divided into two compartments by a heavy but freely moving piston. The piston is clamped in a specified position and the gases in each compartment are prepared in distinct equilibrium states. The piston is then unclamped and the composite system evolves to a global equilibrium. This simple scenario leads to surprisingly complex dynamics that are still incompletely understood, in both the cases where the two gases are elastic [2–5] and where they are inelastic [6]. In the elastic system, the piston moves quickly to establish mechanical equilibrium where the pressures in each compartment are equal. Subsequently, the piston develops oscillations that decay slowly as true thermal equilibrium is achieved [2–5]. For the inelastic system, there is a spontaneous symmetry breaking in which the gas on one side of the piston gets compressed into a solid [6]. Surprisingly, this process is not monotonic, but rather, the piston undergoes oscillatory motion whose period grows exponentially with time.

Given the complexities of these many-body problems, we instead investigate a much simpler version (Fig. 1): a three-particle system [7] in the interval $0 \leqslant x \leqslant 1$ consisting of two light particles of masses $m_1 = m_3 = 1$ that are separated by a heavy piston of mass $m_2 \gg 1$. All interparticle collisions and collisions between particles and the ends of the interval (henceforth termed walls) are elastic. We will develop a simple geometric approach and complementary numerical simulations to help understand the complex dynamical features of this idealized system. These results may ultimately be useful for understanding the many-body piston problem.

An additional motivation to investigate the three-particle system is the connection to the collective behavior in one-dimensional (1D) fluids. The dimensional constraint induces strong interparticle correlations that lead to anomalous transport properties. For example, heat conductivity is generally extremely large for 1D fluids, while mass diffusion is exceedingly slow [8]. An example of a 1D fluid that exhibits such phenomenology is a gas of point particles with alternating masses [9]. This fluid can be viewed a collection of three-particle subsystems, each similar to our idealized model. We therefore anticipate that the dynamics of our three-particle system can shed light on anomalous collective phenomena that arise in 1D fluids.

In the next section, we outline the basic phenomenology of the three-particle system. Then in Sec. III, we map the trajectories of three particles on the line onto an equivalent elastic billiard particle that moves within a highly skewed tetrahedron, with the specular reflection whenever the billiard hits the tetrahedron boundaries [10–14]. From this simple geometrical mapping, we can understand many of the unusual dynamical properties of the system, as will be discussed in Sec. IV. Perhaps the most unexpected feature is the long excursions of the piston close to the walls. By the billiard equivalence, we will argue, in Sec. V, that these long excursions can be understood as the collision point of the billiard in the tetrahedron undergoing a random walk. We will thereby find that the distribution of interval midpoint crossing times by the piston has a power-law tail with exponent $-3/2$.

In an accompanying paper, we will consider the three-particle system when collisions between the light particles and the walls are inelastic. Surprisingly, much of the phenomenology of this idealized three-particle system closely

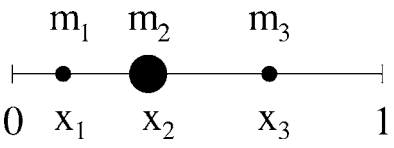

FIG. 1. The three-particle system—a piston and two light particles.

*Email address: phurtado@onsager.ugr.es
†Permanent address: Department of Physics, Boston University, Boston, Massachusetts 02215, USA. Email address: redner@bu.edu

 ©2006 The American Physical Society

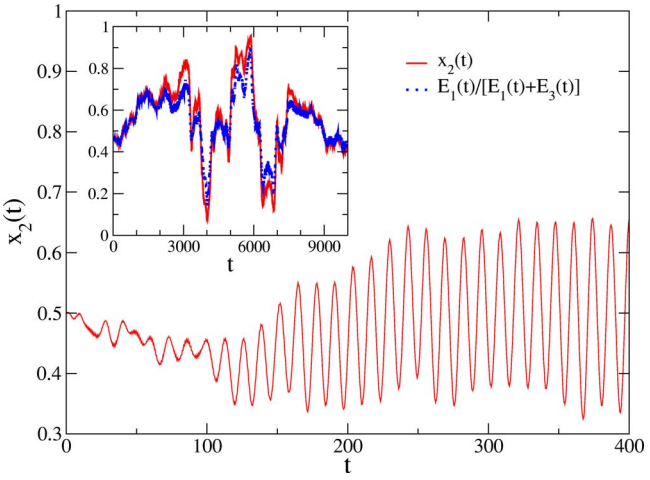

FIG. 2. (Color online) Trajectory of the piston for $t<400$ for $m_2=100$ and initial positions $x_1=0.3$, $x_2=0.5$, and $x_3=0.7636$; note the offset of the vertical axis. Inset: Trajectory for $t<10^4$, as well as the estimate $x_2(t)\approx E_1(t)/[E_1(t)+E_3(t)]$ (see text). These data are averaged over a 400-point range for ease of visualization.

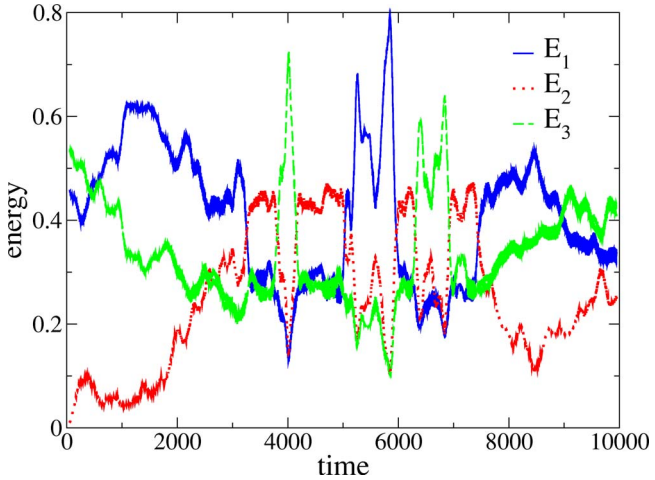

FIG. 3. (Color online) Particle energies as a function of time averaged over a 400-point range.

mirrors the complex dynamics that arises in the many-particle inelastic piston problem [6].

II. PISTON MOTION

To appreciate the basic phenomena, we show a typical piston trajectory obtained numerically in Fig. 2 for the case $m_2=100$. We focus on the case $m_2=100$ because the overall simulation time scales as $\sqrt{m_2}$ and there is already good scaling behavior for $m_2=100$. However, we find qualitatively similar behavior for other values of $m_2\gg 1$. For concreteness and simplicity, we also consider the initial condition in which the light particles approach a stationary piston at $x_2=1/2$ with velocities $v_1=+1$ and $v_3=-1$, so that the total momentum equals 0 while the total energy $E=1$. The initial particle positions of the light particles are uniformly distributed in $(0,1/2)$ and $(1/2,1)$, respectively. Again, we also studied different initial speeds for the light particles and verified that our asymptotic results for the main quantities of interest do not qualitatively depend on the initial conditions.

For the initial condition in which the light particles approach the piston with velocities $v_1=+1$ and $v_3=-1$, we find that after a short transient for $t\lesssim 100$, the piston settles into a quasiperiodic motion with period of $T\approx 12$. This time scale can be understood from simple arguments: if there is energy equipartition, the piston would have energy $1/3$ and speed $|v_2|=\sqrt{2/3m_2}\approx 0.08$. Equipartition also implies that the typical spatial range of all three particles should be equal. These two features lead to a period of the order of 12, in agreement with the data.

In the limit $m_2\to\infty$, it can be shown that the piston position obeys (see Ref. [15] and the Appendix)

$$\frac{d^2x_2(t_s)}{dt_s^2}=\frac{A_1}{x_2^3(t_s)}-\frac{A_3}{[1-x_2(t_s)]^3}, \tag{1}$$

corresponding to a particle moving in an effective potential well $V_{\rm eff}(x)=\frac{1}{2}[A_1x^{-2}+A_3(1-x)^{-2}]$. Here $t_s\equiv t/\sqrt{m_2}$ is a *slow* time variable that is a natural scale for the piston motion, and $A_{1,3}$ are initial condition-dependent constants. For total energy $E=1$, we numerically determine from Eq. (1) that the oscillatory period in slow time coordinates is $T_s\approx 1.285$. Thus a piston with $m_2=100$ should oscillate with period $T=T_s\sqrt{m_2}\approx 12.85$, in excellent agreement with simulations (Fig. 2). Thus this effective potential picture, which formally applies in the limit $m_2\to\infty$, quantitatively accounts for the short-time oscillations of a heavy but finite-mass piston.

For $t\gtrsim 2000$, however, a considerably slower and much less predictable large-amplitude modulation is superimposed on the quasiperiodic oscillations (inset to Fig. 2). When $m_2=100$, the piston eventually approaches to within of 0.05 of each wall. These long-time extreme excursions are reflected in the time dependence of the particle energies (Fig. 3). For $t>2000$, the piston energy fluctuates strongly and is phase locked with $x_2(t)$ during the extreme excursions. Notice also that for $t<2000$ the piston energy is consistently below its average long-time value, indicating the extent of the transient regime.

We may alternatively estimate the piston position by mechanical equilibrium and basic thermodynamics. We write $P_i\ell_i\propto E_i$, where P_i and E_i are, respectively, the pressure and energy associated with particles $i=1,3$, and ℓ_i is the length available to particle i. Assuming mechanical equilibrium, $P_1=P_3$, and using $\ell_1=1-\ell_3=x_2$, we find $x_2(t)=E_1(t)/[E_1(t)+E_3(t)]$. This is very close to the numerical data for $x_2(t)$ (inset to Fig. 2); thus the piston excursions and the large energy fluctuations away from equipartition are closely connected.

Finally, Eq. (1) can be derived heuristically. The equation of motion for the piston is $m_2\dot{v}_2=F_1-F_3$, where the overdot denotes the time derivative and F_i is the force exerted on the piston by particle i. Consider a time range large compared to the typical time between successive light particle bounces, but small compared to the time for the piston to move a unit distance. Then $F_i\approx\Delta p_i/\Delta t_i$, where $\Delta p_i=-\Delta v_i$ is the momentum change of the piston after a collision with particle i, and Δt_i is the time between successive bounces of the particle

with the piston. When particle 1 with velocity v_1, collides with the piston with velocity v_2, the outgoing velocity of the former is $2v_2-v_1$ in the limit $m_2 \gg 1$. Since $v_2 \sim O(m_2^{-1/2})$, we have $\Delta p_1 \approx 2v_1$. Now $\Delta t_1 \approx 2\ell_1/v_1$, where $\ell_1=x_2$ is the length of the subinterval that contains particle 1. Parallel results hold for collisions between the piston and particle 3. Thus

$$m_2\dot{v}_2 = \frac{v_1^2}{x_2} - \frac{v_3^2}{1-x_2}. \tag{2}$$

To obtain v_1, note that after reflection from the left wall, particle 1 approaches the piston with velocity v_1-2v_2, so the net change in v_1 between successive collisions with the piston is $-2v_2$. Thus the velocity of particle 1 evolves according to $\dot{v}_1 \approx -2v_2/(2\ell_1/v_1) = -v_1\dot{x}_2/x_2$, with solution $v_1 \propto 1/x_2$. An analogous equation holds for v_3. Using these results in Eq. (2) gives Eq. (1).

III. BILLIARD MAPPING

To help understand the unusual features of the particle trajectories, it proves useful to follow conventional practice [10–14] and map the three-particle system into an equivalent effective billiard. To be general, suppose that the particles have masses m_1, m_2, and m_3, are located at $0 \leqslant x_1(t) \leqslant x_2(t) \leqslant x_3(t) \leqslant 1$, and have velocities $v_1(t)$, $v_2(t)$, and $v_3(t)$. The trajectories of the three particles in the interval are then equivalent to the trajectory $(x_1(t), x_2(t), x_3(t))$ of an effective billiard particle in the three-dimensional domain defined by the constraints $0 \leqslant x_1 \leqslant x_2 \leqslant x_3 \leqslant 1$. For example, a collision between particle 1 and the left wall corresponds to the billiard ball hitting the boundary $x_1=0$, while a collision between particles 1 and 2 corresponds to the billiard hitting the boundary $x_1=x_2$, etc.

Unfortunately, momentum conservation shows that collisions between the effective billiard and the boundaries of the domain are not specular. Consequently, a naive analysis of successive billiard collisions becomes prohibitively cumbersome. However, a considerable simplification is achieved by introducing the "billiard" coordinates [10–14]

$$y_i = x_i\sqrt{m_i}, \quad w_i = v_i\sqrt{m_i}, \quad i = 1,2,3. \tag{3}$$

In these coordinates, the constraints $x_1 \leqslant x_2$ and $x_2 \leqslant x_3$ become

$$\sqrt{\frac{m_2}{m_1}}y_1 \leqslant y_2, \quad \sqrt{\frac{m_3}{m_2}}y_2 \leqslant y_3,$$

while the constraints involving the walls are $y_1 \geqslant 0$ and $y_3 \leqslant \sqrt{m_3}=1$. As shown in Fig. 4, the allowed region for the billiard is the interior of a highly skewed tetrahedron whose two acute interior angles are given by $\theta = \tan^{-1}\sqrt{1/m_2}$. While this geometry may seem complicated at first sight, these coordinates ensure that all billiard collisions with domain boundaries are specular [12–14], and this feature greatly simplifies the problem.

We now exploit this billiard mapping to characterize the motion of the piston in the original three-particle system. For

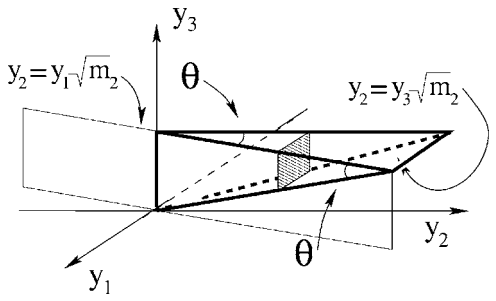

FIG. 4. The allowed tetrahedron (outlined by heavy lines) for the effective billiard particle in y_i coordinates. The back and top planes of the tetrahedron are defined by $y_1=0$ and $y_3=1$, while the planes $y_2=y_1\sqrt{m_2}$ and $y_2=y_3\sqrt{m_2}$ correspond to 1-2 and 2-3 collisions.

a zero-momentum initial condition, the initial billiard trajectory lies within the shaded square $y_2=\sqrt{m_2}/2$ (equivalent to $x_2=1/2$ in the interval) in Fig. 4. If the first collision is between the piston and particle 1, the equivalent billiard first hits the front wall of the tetrahedron. Because of specularity, the billiard is reflected toward increasing y_2. Conversely, if the first collision is between the piston and particle 3, the billiard first hits the bottom wall and the reflected trajectory is toward decreasing y_2.

The opposite effects of successive 1-2 and 2-3 collisions lead to the billiard persisting close to the shaded square $y_2=\sqrt{m_2}/2$. However, once the billiard develops a nonzero velocity in the y_2 direction, the trajectory is unlikely to return to the initial square. Subsequently, the billiard bounces back and forth primarily along the y_2 direction in the tetrahedron, corresponding to the quasiperiodic oscillations in the interval shown in Fig. 2. At still longer times, the billiard motion consists of unpredictable modulations that are superimposed on the quasiperiodic oscillations. The long-lived excursions of the piston near one end of the interval correspond to the billiard remaining close to one of the acute-angled ends of the tetrahedron in Fig. 4.

Another useful consequence of the billiard mapping is that we can also deduce in simple terms the probability distribution $\pi_2(x)$ for finding the piston at position $x_2=x$ in the interval, or equivalently the probability for finding the billiard with coordinate $y_2=x_2\sqrt{m_2} \equiv z$. This distribution can also be found by using the microcanonical ensemble (see, e.g., the first paper in Ref. [7]). If the billiard covers the tetrahedron equiprobably, then $\pi_2(x)$ would be proportional to the area of the rectangle defined by the intersection of the plane $y_2=z$ and the tetrahedron in Fig. 4. This mixing property is believed to occur in triangular billiards with irrational angles [16] and also in various three-dimensional billiard geometries [17]. Given that the angles of our tetrahedron generically are irrational except for particular values of m_2, we expect that billiard trajectories in this tetrahedron will also be mixing.

From this mixing hypothesis, $\pi_2(z)$ is simply proportional to the area of the rectangle $y_2=z$ in the tetrahedron. Now the length of the horizontal side of the rectangle is proportional to $z/\sqrt{m_2}$, while the length of the vertical side is proportional to $1-z/\sqrt{m_2}$. Thus the rectangle area is proportional to

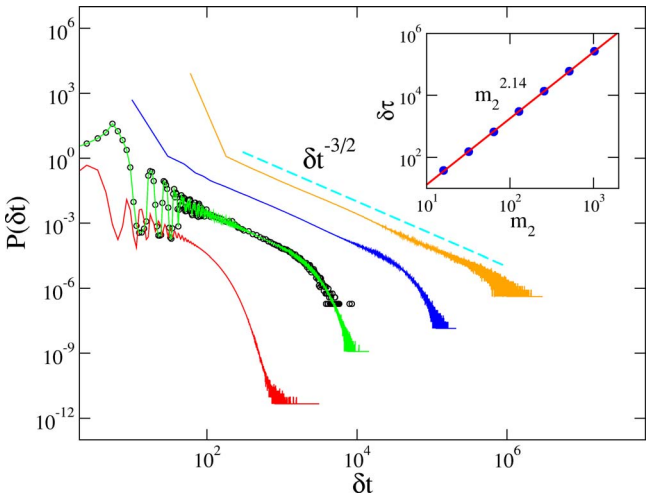

FIG. 5. (Color online) The distribution of midpoint crossing time intervals $P(\delta t)$ for $m_2=2^n$, with $n=4,6,8$, and 10 on a double logarithmic scale (lower to upper curves) for zero initial momentum of the system. For the case $m=64$, we also show as open circles the distribution for random initial conditions (positions and velocities) of the light particles. For visibility, each successive curve is shifted vertically upward by 10^{n-4}. Early-time oscillations do not appear for large m_2 because the histogram bin is larger than interpeak spacing in Fig. 6. Inset: The cutoff $\delta\tau$ as a function of m_2.

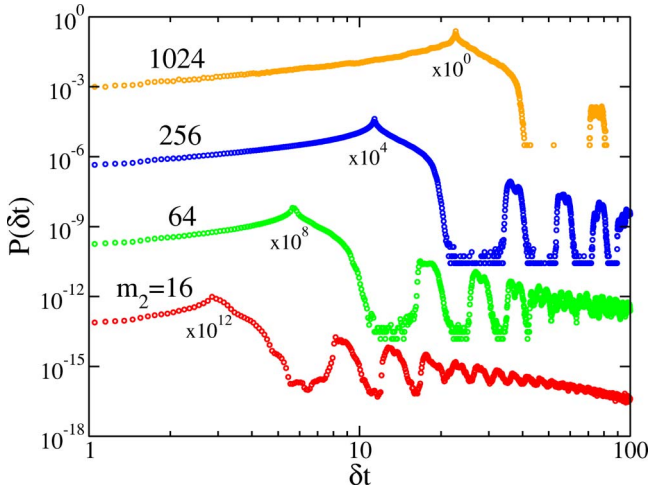

FIG. 6. (Color online) The short-time behavior of $P(\delta t)$ for different m_2.

$z/\sqrt{m_2}(1-z/\sqrt{m_2})=x_2(1-x_2)$. Normalization of this probability fixes the proportionality constant and we thus obtain $\pi_2(x)=6x(1-x)$ for the probability that the piston is located at x. Similarly, the position distribution of the light particles is found by computing the areas of the triangles defined by the intersection of the planes $y_i=x\sqrt{m_i}$ $(i=1,3)$ with the tetrahedron. This leads to $\pi_1(x)=3(1-x)^2$ and $\pi_3(x)=3x^2$.

We tested these predictions numerically and obtained excellent agreement between the above theoretical expectations and the simulation results. Notice that under the assumption of the billiard visiting all points in the tetrahedron equiprobably, the probability of finding *any* particle at a given position on the interval is a constant; that is, $\Pi(x)\equiv\frac{1}{3}\Sigma_i\pi_i(x)=1$.

IV. EXTREME EXCURSIONS

To characterize the wanderings of the piston near the ends of the interval, we study the probability distribution $P(\delta t)$ to have a time interval δt between successive midpoint crossings by the piston. A midpoint crossing corresponds to the equivalent billiard crossing the plane $y_2=\sqrt{m_2}/2$. As shown in Fig. 5, $P(\delta t)$ decays as the power law $(\delta t)^{-\mu}$ over a significant time range. For the case of $m_2=1024$, the data for $P(\delta t)$ versus δt are quite linear on a double logarithmic scale for δt in the range $[1.8\times10^2, 3.1\times10^5]$. We measure the slope to be $\mu=1.5203\pm0.0024$. At longer times, the data have an exponential cutoff $P(\delta t)\sim e^{-\delta t/\delta\tau}$, where $\delta\tau\sim m_2^{\lambda}$ with $\lambda=2.14\pm0.01$ (inset to Fig. 5). Correspondingly, the average time between crossings varies as $\langle\delta t\rangle\sim m_2^{(2-\mu)\lambda}$.

From the relation $x_2(t)\approx E_1(t)/[E_1(t)+E_3(t)]$ derived in Sec. II, the piston crosses the midpoint whenever $E_1(t)=E_3(t)$; thus $P(\delta t)$ can also be interpreted as the probability that the inequality $E_1(t)\neq E_3(t)$ persists for a time δt. This long-time persistence of energy asymmetry is in agreement with previous simulations of 1D binary fluids [9], in which light particles were reported to trap energy and release it very slowly.

The early-time sequence of peaks in $P(\delta t)$ is simply related to the half-period of the short-time piston oscillations (and its resonances), $\frac{1}{2}T=\frac{1}{2}T_s\sqrt{m_2}$, where $T_s\approx1.285$ is the slow-time period associated with a particle in the effective potential of Eq. (1). Thus the first peak of $P(\delta t)$ should be at $\delta t\approx2.6$, 5.1, 10.3, and 20.6 for $m_2=16$, 64, 256, and 1024, respectively, very close to the results in Fig. 6.

To understand the long-time power-law in $P(\delta t)$, we show in Fig. 7 the particle trajectories from Fig. 2 during the extreme excursion near $t\approx4000$. This excursion is driven by a sequence of nearly periodic oscillations due to precisely orchestrated correlated motion of the lighter particles. Consider first the collisions between particle 1 and the piston when the latter moves toward $x=0$. There is a violent series of "rat-

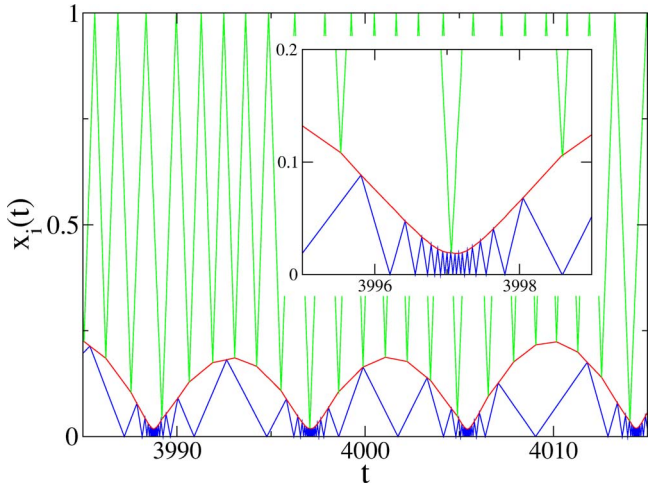

FIG. 7. (Color online) Positions of the three particles for the system of Fig. 2 near $t=4000$. Inset: Finer detail near $t=3997$.

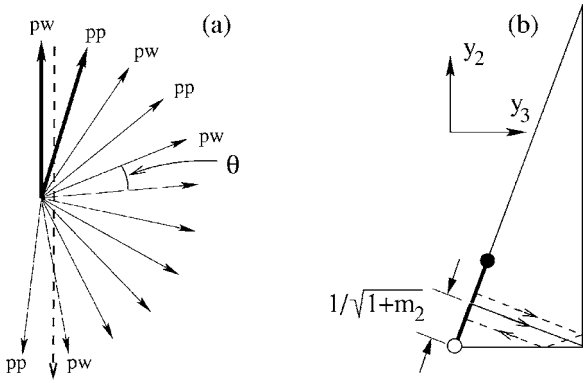

FIG. 8. (a) The wedge that represents collisions between particle 1, the piston, and the left wall in billiard coordinates (thick lines). Lighter lines show the periodic extension of wedge. The dashed straight line is periodic extension of the billiard trajectory. (b) The billiard after projection from the tetrahedron onto the y_2-y_3 triangle. Shown is the periodic trajectory when the piston and particle 3 have equal and opposite momenta and meet at $x=1/(1+m_2)$. A two-cycle arises (dashed) when the collision point deviates within the thick segment of the hypotenuse while the particle momenta remain equal and opposite.

tling" collisions as the piston first approaches $x=0$ and ultimately is reflected [14,18]. In the limit $m_2 \gg 1$, these rattling collisions are equivalent to the piston having a nearly elastic reflection from the wall. After this rattling collision, the piston is met by particle 3 whose momentum is of a similar magnitude, but opposite to that of the piston. Thus after a few collisions between the piston and particle 3 (seven such collisions in Fig. 7) the piston is reflected back toward $x=0$, where the rattling between particle 1 and the piston recurs.

V. EFFECTIVE RANDOM WALK DESCRIPTION

To determine $P(\delta t)$ from this descriptive account of the rattling collisions, we consider a reduced problem in which the fastest degrees of freedom associated with particle 1 are integrated out. As we shall show, the slower degree of freedom associated with the piston can then be described qualitatively by an effective random walk. This then allows us to deduce the statistics of the time between successive piston crossings of the interval midpoint.

For the piston to persist near the left wall, the collisions between the piston and particle 3 must be close to periodic. A deviation from periodicity occurs because the net effect of the rattling between particle 1 and the piston is a slightly inelastic collision. We now estimate the departure from elasticity in these rattling collisions and we then use this result to estimate the duration of the resonance between the piston and particle 3.

In billiard coordinates, the rattling collision can be represented as the effective billiard entering a narrow wedge of opening angle $\theta=\tan^{-1}(1/\sqrt{m_2})$ [Fig. 8(a)] that is the projection of the tetrahedron onto the y_1-y_2 plane. Because each collision of the billiard with the wedge is specular, the ensuing rattling sequence is equivalent to a straight trajectory in the periodic extension of the wedge [Fig. 8(a)]. Each collision is alternately particle-particle and particle-wall, so that the identity of periodically extended barriers alternates between *pp* and *pw*. The rattling sequence ends when the billiard trajectory no longer crosses a wedge boundary. The crucial point is that the final billiard velocity vector deviates by no more than an angle θ with respect to the two rays that define the last wedge.

Suppose that the initial velocity vector is $\vec{v}^{(i)} \equiv (v_1, v_2) = (0,-1)$, corresponding to $\vec{w}^{(i)} \equiv (w_1, w_2) = (0, -\sqrt{m_2})$. If the final billiard trajectory is parallel to a *pw* boundary in Fig. 8(a), then $\vec{v}^{(f)}$ is $(0,+1)$. This corresponds to a rattling sequence in which particle 1 begins and ends at rest and the piston is elastically reflected. Conversely, if the final trajectory is parallel to a *pp* boundary, then

$$\vec{w}_f = \sqrt{m_2/(1+m_2)}(-1, -\sqrt{m_2})$$

(note that $w_i^2 = w_f^2$). Translating to original coordinates, the minimum final piston speed is $\sqrt{m_2/(1+m_2)}$. Therefore rattling collisions lead to a final piston velocity that lies within the narrow range $(1-1/2m_2, 1)$ for $m_2 \gg 1$.

From this deviation from elasticity, we determine the time needed to disrupt the resonance between the piston and particle 3. Consider the two-particle system consisting of the piston and particle 3 with initial velocities $(v_2, v_3) = (1/m_2, -1)$ and with $x_2 = x_3 = x = 1/(1+m_2)$. This resonant starting state ensures that the two particles hit the opposite ends of the interval simultaneously and then meet again at $x=1/(1+m_2)$ with $(v_2, v_3) = (1/m_2, -1)$ when all collisions are elastic. In billiard coordinates this periodic motion translates to a singular trajectory in the projection of the tetrahedron onto the y_2-y_3 plane [Fig. 8(b)]. A 2-3 collision corresponds to the billiard hitting the hypotenuse of the resulting triangle perpendicularly and the simultaneous collision of the particles with the interval ends corresponds to the billiard hitting at the right-angle corner of the triangle. If the initial position slightly deviates from $x=1/(1+m_2)$ while the initial velocities are on resonance, then the subsequent motion is simply a two-cycle, as indicated in the figure.

Now consider the influence of particle 1 on this resonance. Due to the slight inelasticity of the effective collision between the piston and the left wall, the speed of the reflected piston changes stochastically by the order of m_2^{-1}. Consequently, the 2-3 collision point shifts from $x=1/(1+m_2)$ to $x=1/(1+m_2) \pm O(1/m_2^2)$. In billiard coordinates, the return trajectory in Fig. 8(b) is not exactly parallel to the initial trajectory and the collision point on the hypotenuse moves stochastically by an amount of the order of $m_2^{-3/2}$. When this collision point moves outside the thick line in Fig. 8, the resonance between the piston and particle 3 terminates and the piston crosses the interval midpoint shortly thereafter.

Thus the collision point on the hypotenuse undergoes a random walk on an interval of length $O(m_2^{-1/2})$ with one end absorbing (open circle in Fig. 8) and the other end reflecting (solid dot). The probability that the billiard remains in this interval up to time δt therefore scales as $P(\delta t) \sim \delta t^{-3/2}$ until an exponential cutoff because of the finiteness of the interval [19]. The cutoff time should be L^2/D, where $L \sim O(m_2^{-1/2})$ is

the interval length and $D \propto [O(m_2^{-3/2})]^2$ is the diffusion coefficient associated with individual random-walk steps of length $m_2^{-3/2}$. This leads to a cutoff time $\delta\tau \sim m_2^2$, consistent with the simulation result $\delta\tau \sim m_2^{2.14}$ shown in Fig. 5.

VI. DISCUSSION

We introduced a toy version of the classic piston problem in which a massive particle (the piston) separates a finite interval into two compartments, each containing a single light particle. In spite of its simplicity, the dynamics of this 3-particle system is surprisingly rich. When all collisions are elastic, the piston undergoes complex motion, with short-time quasiperiodic behavior and seemingly chaotic behavior at long times. The early-time can be understood in terms of the piston oscillating in an effective potential well $V_{\rm eff} = [A_1 x^{-2} + A_3 (1-x)^{-2}]$. To understand the long-time behavior, we mapped the motion of three particles in the interval onto that of an effective equivalent billiard in a tetrahedral domain. We then used geometric methods that help explain some of the anomalous dynamical features of the piston.

At long times, the piston moves in an apparently unpredictable fashion, with long-lived excursions close to the ends of the interval during which large departures from energy equipartition occur. We quantified these extreme excursions by studying the distribution of time intervals for the piston to cross the interval midpoint. This distribution has a power-law decay over a wide time range, with exponent $-3/2$. We argued that this phenomenon can be recast as a first-passage problem of a random walk within a finite interval, leading naturally to the above exponent value.

Although individual trajectories of the piston seem unpredictable, average properties are considerably simpler. We found a simple form for the probability distribution $\pi_i(x)$ for finding particle i at position x; namely, $\pi_1(x) = 3(1-x)^2$, $\pi_2(x) = 6x(1-x)$, and $\pi_3(x) = 3x^2$. These forms are a direct consequence of the billiard trajectory being mixing in the tetrahedron.

The three-particle system studied in this work is clearly oversimplified to faithfully model a many-particle piston system in three dimensions. Nevertheless, the methods developed here may prove useful in understanding few-particle elastic or granular systems and may help suggest new approaches to deal with many-particle systems in higher dimensions.

ACKNOWLEDGMENTS

We thank R. Brito for collaboration during the initial stages of this project. S.R. thanks NSF Grant No. DMR0227670 (BU) and DOE Grant No. W-7405-ENG-36 (LANL) for financial support. P.I.H. acknowledges support from Spanish MEC, and thanks LANL and CNLS for hospitality during part of this project.

APPENDIX: EFFECTIVE POTENTIAL FOR AN INFINITE-MASS PISTON

Here we show that Eq. (1) governs the piston motion in the limit $m_2 \to \infty$ by specializing the general result of Sinai [15] to the three-particle elastic system in the interval. We assume a initially at $x_2(0) = 1/2$ with $v_2(0) = 0$, and unit-mass particles 1 and 3 starting at random positions to the left and right of the piston, respectively, with velocities $v_1(0) = +1$ and $v_3(0) = -1$. Energy conservation implies that $|v_2(t)| < \sqrt{2/m_2}$. It is then natural to define a slow time variable, $t_s = t/\sqrt{m_2}$, such that the piston velocity is $O(1)$ in this time scale.

Consider an infinitesimal slow time interval $[t_s, t_s + \delta]$ during which the piston moves a distance $O(\delta)$, while the number of 1-2 and 2-3 collisions is $O(\sqrt{m_2})$. Let k index each piston collision; we define this collision index to run from $k_- + 1$ to k_+ in $[t_s, t_s + \delta]$. The total number of collisions experienced by the piston in this time range is $N = k_+ - k_-$. The particle velocities just before each collision with the piston are given by

$$v_2(k) = (1-\epsilon) v_2(k-1) + \epsilon v_i(k-1), \tag{A1}$$

$$v_i(k) = (\epsilon - 1) v_i(k-1) + \alpha v_2(k-1), \tag{A2}$$

where $\epsilon = 2/(1+m_2)$, $\alpha = \epsilon m_2$, $i = 1, 3$, and $v(k)$ is a particle velocity just before the $(k+1)$st piston collision. For large piston mass recollisions do not occur, that is, light particles always hit a boundary before colliding again with the piston. Therefore, $v_1(k) > 0$ and $v_3(k) < 0 \ \forall \ k \in [k_-, k_+ - 1]$.

Next we iterate the first term in Eq. (A1) to write $v_2(k_+) \equiv v_2(t_s + \delta)$ in terms of $v_2(k_-) \equiv v_2(t_s)$. Let n_{12} and n_{23} be the number of 1-2 and 2-3 collisions in the sequence $k_- + 1, \ldots, k_+$, respectively, with $N = n_{12} + n_{23}$. For $i \in [1, n_{12}]$, we define $c_1(i) = k$ if and only if the ith 1-2 collision corresponds to the kth collision in $k_- + 1, \ldots, k_+$, so that $c_1(i) \in [1, N]$ and similarly for $c_3(j)$, with $j \in [1, n_{23}]$. With these definitions, (A1) gives

$$v_2(k_+) = (1-\epsilon)^N v_2(k_-) + \epsilon \sum_{i=1}^{n_{12}} (1-\epsilon)^{N - c_1(i)} v_1[k_- + c_1(i) - 1] + \epsilon \sum_{i=1}^{n_{23}} (1-\epsilon)^{N - c_3(i)} v_3[k_- + c_3(i) - 1]. \tag{A3}$$

The piston velocity in the slow time variable is $w_2(t_s) \equiv dx_2/dt_s = \sqrt{m_2} v_2(t_s)$. To derive a closed equation for $w_2(t_s)$, we first take the limit $m_2 \to \infty$ and then $\delta \to 0$. Using the definition of $w_2(t_s)$ and Eq. (A3), we find

$$\begin{aligned} w_2(t_s + \delta) - w_2(t_s) &= [(1-\epsilon)^N - 1] w_2(t_s) + \epsilon \sqrt{m_2} \Bigg(\sum_{i=1}^{n_{12}} [(1-\epsilon)^{N - c_1(i)} - 1] \\ &\quad \times v_1[k_- + c_1(i) - 1] + \sum_{j=1}^{n_{23}} [(1-\epsilon)^{N - c_3(j)} - 1] \\ &\quad \times v_3[k_- + c_3(j) - 1] + \sum_{i=1}^{n_{12}} v_1[k_- + c_1(i) - 1] \\ &\quad + \sum_{j=1}^{n_{23}} v_3[k_- + c_3(j) - 1] \Bigg). \end{aligned} \tag{A4}$$

We expand this expression for $m_2 \to \infty$, taking into account that $\epsilon \sim O(m_2^{-1})$ and $n_{1,3} \sim O(\sqrt{m_2})$, to obtain

$$w_2(t_s+\delta) - w_2(t_s) = \epsilon\sqrt{m_2}\left(\sum_{i=1}^{n_{12}} v_1[k_- + c_1(i) - 1] + \sum_{j=1}^{n_{23}} v_3[k_- + c_3(j) - 1]\right) + O\left(\frac{1}{\sqrt{m_2}}\right). \tag{A5}$$

Because the large piston mass causes the light particle velocities to change only slightly in the slow time interval $[t_s, t_s+\delta]$, we can write

$$\sum_{k=1}^{n_i} v_i[k_- + c_i(k) - 1] \approx n_i v_i(t_s) \tag{A6}$$

for $i=1,3$, with $v_i(t_s) \equiv v_i(k_-)$, and where correction terms vanish as $\delta \to 0$ [15]. Within this approximation of nearly constant light-particle velocities, the unscaled time intervals between successive 1-2 and 2-3 collisions are $2x_2(t_s)v_1^{-1}(t_s)$ and $-2[1-x_2(t_s)]v_3^{-1}(t_s)$, respectively. Thus

$$n_{12} \approx \frac{v_1(t_s)\sqrt{m_2}\delta}{2x_2(t_s)}, \quad n_{23} \approx \frac{-v_3(t_s)\sqrt{m_2}\delta}{2(1-x_2(t_s))},$$

with $v_1(t_s) > 0$ while $v_3(t_s) < 0$. Using these results in Eq. (A5), we obtain, in the asymptotic limit,

$$\frac{dw_2(t_s)}{dt_s} = \frac{v_1^2(t_s)}{x_2(t_s)} - \frac{v_3^2(t_s)}{[1-x_2(t_s)]}. \tag{A7}$$

We now derive the equation of motion for $v_i(t_s)$, $i=1,3$. Here we consider only particle 1, since the derivation for particle 3 is analogous. Let us introduce a new index $q \in [1, n_{12}]$, such that $v_1(q)$ and $v_2(q)$ are the velocities of particle 1 and the piston just before the $(q+1)$st 1-2 collision (notice a subtle difference from the previous notation; between the qth and the $(q+1)$st 1-2 collisions, the piston may collide one or more times with particle 3). From Eq. (A2) we have

$$v_1(q+1) = (1-\epsilon)v_1(q) - \alpha v_2(q).$$

Notice the extra minus sign in this equation compared to Eq. (A2) to account for the reflection of the light particle off the wall. Iterating this equation, we find

$$v_1(n_{12}) = (1-\epsilon)^{n_{12}} v_1(0) - \alpha \sum_{q=0}^{n_{12}-1} (1-\epsilon)^{n_{12}-q-1} v_2(q),$$

where now $v_1(n_{12}) \equiv v_1(t_s+\delta)$ and $v_1(0) \equiv v_1(t_s)$. Taking the limit $m_2 \to \infty$ now yields

$$v_1(t_s+\delta) - v_1(t_s) = -2\sum_{q=0}^{n_{12}-1} v_2(q) + O\left(\frac{1}{\sqrt{m_2}}\right).$$

We now write $v_2(q)$ as $v_2(0) + \sum_{k=1}^{q}[v_2(k) - v_2(k-1)]$. Therefore,

$$\sum_{q=0}^{n_{12}-1} v_2(q) = n_{12}v_2(0) + \sum_{q=0}^{n_{12}-1}\sum_{k=1}^{q}[v_2(k) - v_2(k-1)]. \tag{A8}$$

The double sum in Eq. (A8) can be demonstrated to be $O(\delta^2)$ [15], so it is negligible in the $\delta \to 0$ limit. Therefore

$$v_1(t_s+\delta) - v_1(t_s) = -\frac{\delta v_1(t_s)\sqrt{m_2}}{x_2(t_s)} v_2(t_s) + O(\delta^2).$$

Finally, for $m_2 \to \infty$ and $\delta \to 0$ we find

$$\frac{dv_1(t_s)}{dt_s} = -\frac{v_1(t_s)}{x_2(t_s)}\frac{dx_2}{dt_s},$$

$$\frac{dv_3(t_s)}{dt_s} = \frac{v_3(t_s)}{1-x_2(t_s)}\frac{dx_2}{dt_s}. \tag{A9}$$

Integrating these equations yields $v_1(t_s) = B_1/x_2(t_s)$ and $v_3(t_s) = B_3/[1-x_2(t_s)]$, with $B_{1,3}$ constants which depend on the initial condition. Using these solutions in Eq. (A7) we finally arrive at the piston equation of motion given in Eq. (1).

[1] H. B. Callen, *Thermodynamics* (J. S. Wiley & Sons, New York, 1960).

[2] E. H. Lieb, Physica A **263**, 491 (1999).

[3] E. Kestemont, C. Van den Broeck, and M. Malek Mansour, Europhys. Lett. **49**, 143(2000).

[4] C. Gruber, S. Pache, and A. Lesne, J. Stat. Phys. **108**, 669 (2002); **112**, 1177 (2003).

[5] N. I. Chernov, J. L. Lebowitz, and Ya. G. Sinai, Russ. Math. Surveys **57**, 1045 (2002).

[6] R. Brito, M. J. Renne, and C. Van den Broeck, Europhys. Lett. **70**, 29 (2005).

[7] For related investigations of the dynamics of three-particle elastic systems, see, e.g., J. Rouet, F. Blasco, and M. R. Feix, J. Stat. Phys. **71**, 209 (1993); S. L. Glashow and L. Mittag, *ibid.* **87**, 937 (1996); S. G. Cox and G. J. Ackland, Phys. Rev. Lett. **84**, 2362 (2000).

[8] S. Lepri, R. Livi, and A. Politi, Phys. Rep. **377**, 1 (2003).

[9] A. Dhar, Phys. Rev. Lett. **86**, 3554 (2001); P. L. Garrido, P. I. Hurtado, and B. Nadrowski, *ibid.* **86**, 5486 (2001); A. V. Savin, G. P. Tsironis, and A. V. Zolotaryuk, *ibid.* **88**, 154301 (2002); P. Grassberger, W. Nadler, and L. Yang, *ibid.* **89**, 180601 (2002); P. I. Hurtado, Phys. Rev. E **72**, 041101 (2005); Phys. Rev. Lett. **96**, 010601 (2006).

[10] G. Galperin and A. Zemlyakov, *Mathematical Billiards* (Nauka, Moscow, 1990) (in Russian).

[11] V. V. Kozlov and D. V. Treshshëv, *Billiards: A Generic Introduction to the Dynamics of Systems with Impacts* (American Mathematical Society, Providence, RI, 1991).

[12] S. Tabachnikov, *Billiards* (Société Mathématique de France American Mathematical Society, Providence, RI, 1995).
[13] E. Gutkin, J. Stat. Phys. **81**, 7 (1996).
[14] S. Redner, Am. J. Phys. **72**, 1492 (2004).
[15] Ya. G. Sinai, Theor. Math. Phys. **121**, 1351 (1999).
[16] G. Casati and T. Prosen, Phys. Rev. Lett. **83**, 4729 (1999).
[17] Ya. G. Sinai, Russ. Math. Surveys **25**, 137 (1970).
[18] This problem was apparently first posed by Sinai. See, e.g., Ya. G. Sinai, *Introduction to Ergodic Theory* (Princeton University Press, Princeton, NJ, 1978).
[19] S. Redner, *A Guide to First-Passage Processes* (Cambridge University Press, New York, 2001).